molecules

MDPI

Article

Quality Research on Indigo Naturalis Prepared Using a Novel Method and Preliminary Investigation of Its Anti-Tumor Activity

Xianxiang Xu *, Xinyi Zhou, Lin Lin, Yaling Zhu, Yiting Qiu, Xiaoping Huang, Huiyong Yang, Fei Qiu and Yong Diao *

School of Medicine, Huaqiao University, 269 Chenghua North Road, Quanzhou 362021, China
* Correspondence: xuxianxiang@hqu.edu.cn (X.X.); diaoyong@hqu.edu.cn (Y.D.)

Abstract

The traditional manufacturing process of Indigo Naturalis (IN) adopts lime-mediated indigo beating, which often introduces residual inorganic impurities and yields low contents of bioactive constituents. Herein, we developed an improved preparation protocol using sodium hydroxide to replace calcium hydroxide. The novel-prepared Indigo Naturalis (NIN) exhibited a 10–20-fold increase in indigo content and a 20–30-fold elevation in indirubin content relative to conventionally standard processed IN (SIN). In the present study, systematic quality comparison was performed between NIN and SIN. Nine shared constituents were identified, namely indigo, indirubin, isatin, tryptanthrin, hydroxyindirubin, valine, isorhamnetin, 5, 7, 4′-trihydroxy-8-methoxyflavone, and 2-(1H-indol-3-yl) acetamide. A comprehensive quality control strategy for NIN was established, covering macroscopic characterization, qualitative identification, physicochemical testing, quantitative assay, and characteristic chromatographic fingerprinting. Furthermore, three tumor cell lines (K562, HL-60 and SW480) were employed to test the anti-tumor activities of NIN and SIN. Within a concentration of 0.02–0.32 mg/mL in vitro, NIN inhibited the viability of three tumor cell lines, with a more pronounced effect than SIN, which only inhibited the viability of SW480 cells. Collectively, our findings demonstrate that NIN possesses more pronounced physicochemical quality and superior anti-tumor potential.

Keywords: Qingdai; indigo naturalis prepared using a novel method (NIN); quality analysis; anti-tumor

Academic Editors: Ebru Kurtulbaş and Selin Şahin

Received: 18 October 2026
Revised: 18 November 2026
Accepted: 20 November 2026
Published: 23 November 2026

Copyright: © 2026 by the authors. Licensee MDPI, Basel, Switzerland. This article is an open access article distributed under the terms and conditions of the Creative Commons Attribution (CC BY) license.

1. Introduction

As reflected in the ancient Chinese proverb "Blue is taken from the indigo plant, yet bluer than the plant itself" (青出于蓝而胜于蓝) (dating back to the 3rd century B.C.), indigo plants have long been exploited for natural indigo dye [1]. During traditional indigo manufacturing, precipitated indigo sludge is collected for dyeing purposes, while the floating foam, known as "indigo flower", is harvested as the herbal medicine Qingdai (Indigo Naturalis, IN) [2]. Since the 7th century A.D., IN has been clinically applied for its anti-tumor, anti-bacterial, anti-inflammatory and anti-psoriatic properties [3]. Accumulating evidence reveals that multiple bioactive ingredients from IN, not limited to indirubin, including indigo, tryptanthrin and isatin, exhibit promising therapeutic potential for cancer, ulcerative colitis, psoriasis, infectious and inflammatory disorders [4–

10]. Formulations containing IN, such as realgar–Indigo Naturalis preparation, Qinghuang powder, IN-processed *Ophiopogon japonicus* and curcumin–QingDai combinations, display broad application prospects and provide experimental support for the clinical utilization of IN [11–15].

Conventional IN production consists of plant soaking, lime-assisted indigo beating and water levigation. Nevertheless, marker compounds including indirubin and indigo are present at low levels in the final IN products. Moreover, the use of lime leads to significant quality inconsistencies and compromises therapeutic efficacy. Originating from Fujian Province and derived from *Baphicacanthus cusia* Bremek., Jian-Qingdai represents the premium grade of domestic IN resources [16,17]. Our research group previously reported a lime-free innovative processing technology for IN. From *Baphicacanthus cusia* Bremek., IN prepared using a novel method (NIN) showed protective effects against ulcerative colitis (UC) and exerted favorable bioactivity against inflammatory and malignant colonic cells [18,19]. On this basis, the current work performs comparative quality profiling between NIN and commercially available standard IN (SIN), and preliminarily investigates their anti-tumor activities.

2. Results and Discussion

2.1. Macroscopic Characteristics of NIN

NIN appears as blue-black, lightweight, dust-prone fine powder (Figure 1). It possesses a faint odor and bland taste.



(**A**) (**B**)

Figure 1. From *Baphicacanthus cusia* to NIN ((**A**) raw herb of *Baphicacanthus cusia*; (**B**) final NIN powder).

2.2. Combustion Identification

Upon gentle ignition on aluminum foil, NIN generated purplish-red smoke (Figure 2).

When NIN powder was subjected to gentle ignition on an aluminum foil substrate, purplish-red smoke was released from the sample, and the combustion behavior was visually observed.



Figure 2. Combustion identification of NIN (NIN powder was ignited on aluminum foil, producing characteristic purplish-red smoke).

2.3. Nitric Acid Identification

Dropwise addition of nitric acid onto NIN produced yellow-brown foaming (Figure 3).

When concentrated nitric acid was introduced dropwise onto the NIN powder, a vigorous reaction ensued, accompanied by the formation of yellow-brown foam. The rate of foaming and color change in the reaction system were visually documented.

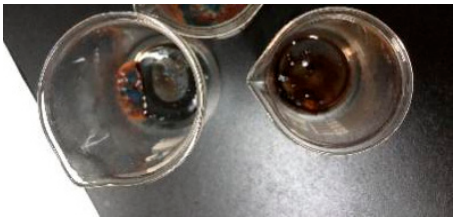

Figure 3. Nitric acid identification of NIN (concentrated nitric acid was added dropwise to NIN powder, and yellow-brown foaming was observed in the reaction system).

2.4. Moisture Inspection

Eight batches of NIN samples were subjected to moisture testing (Table 1). The moisture content of all batches was below 6.82%.

Table 1. Moisture determination of NIN samples (n = 8).

Batch No.	**201801**	**201802**	**201803**	**201804**	**201805**	**201806**	**201807**	**201808**
Moisture (%)	6.37	5.84	4.73	5.51	6.82	4.29	5.23	6.30

2.5. Water-Soluble Pigment Inspection

After overnight standing, the supernatant presented a light-blue color (Figure 4).

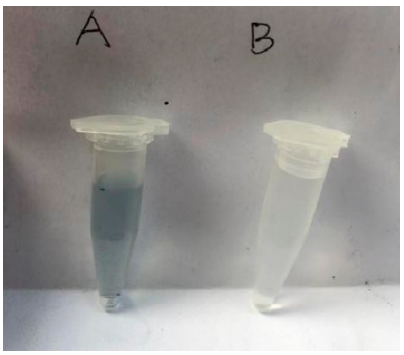

Figure 4. Water-soluble pigment test (the solubility difference in pigments was compared. (**A**) NIN supernatant; (**B**) water blank control).

2.6. High-Performance Liquid Chromatography (HPLC) Fingerprint Chromatogram

By comparing chromatograms of mixed indigo–indirubin reference standards (Figure 5I), peak 4 in Figure 5II was assigned to indigo and peak 9 to indirubin. A total of eleven common peaks were shared by SIN and NIN, among which six minor peaks exhibited peak areas below 100 mAU and five major peaks showed peak areas above 100 mAU. These results suggest high similarity in chemical composition between NIN and SIN.

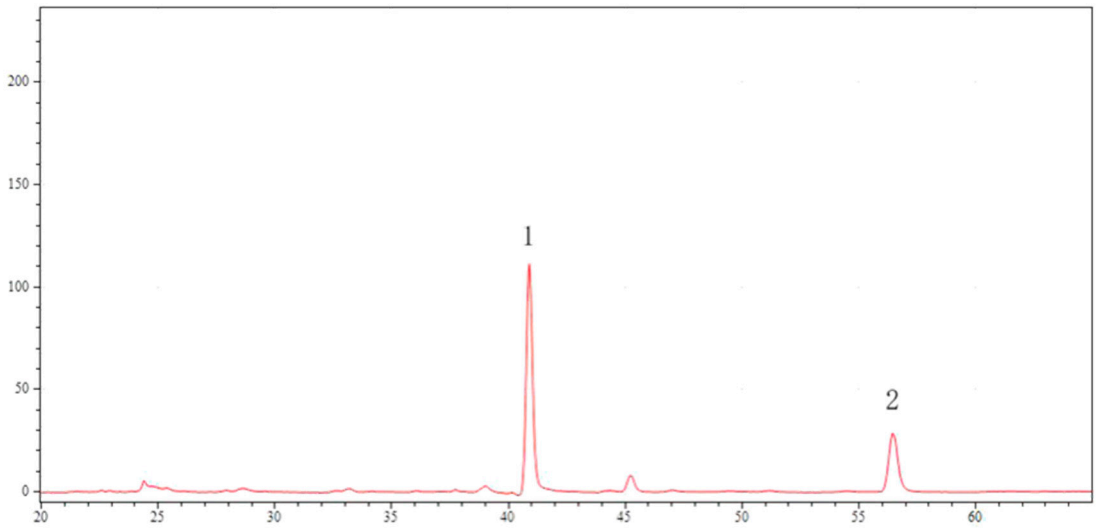

(**I**)

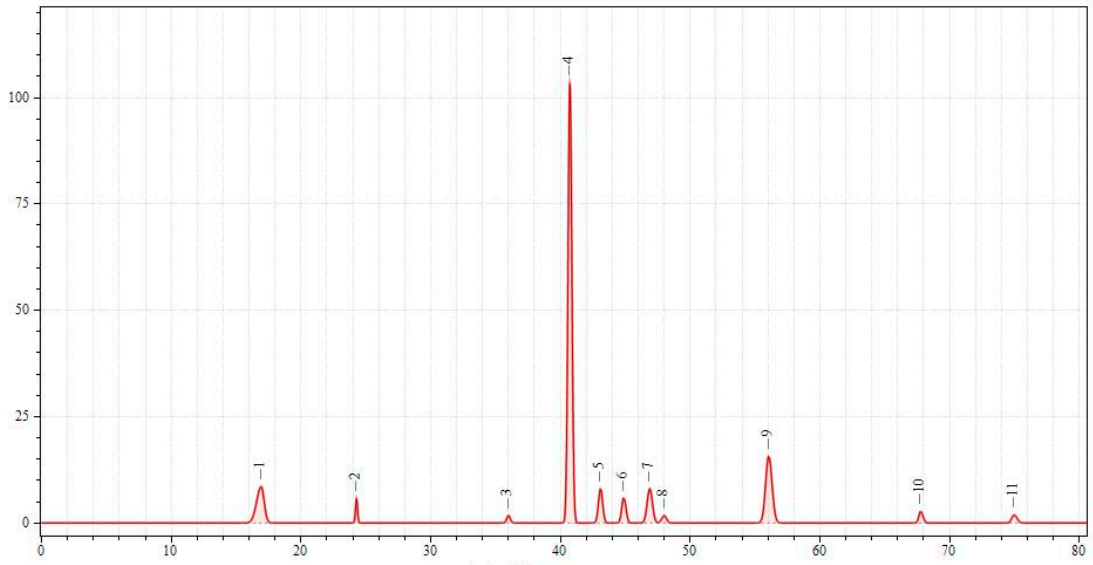

(**II**)

Figure 5. (**I**) HPLC of mixed reference standards of indigo and indirubin (*X*-axis: retention time (min); *Y*-axis: UV absorbance (mAU)); (**II**) HPLC fingerprint common pattern for SIN and NIN (*X*-axis: retention time (min); *Y*-axis: UV absorbance (mAU)).

2.7. Ultra-Performance Liquid Chromatography (UPLC) Profile and Total Ion Chromatogram

Based on retention time matching (Figure 6I,II), quasi-molecular ion peaks (Figure 6III,IV), fragment ion information and the published literature on IN constituents, nine common components were unambiguously identified (Figure 6V).

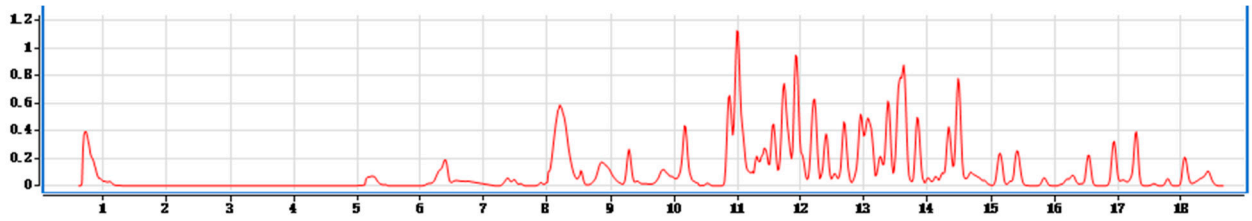

(**I**)

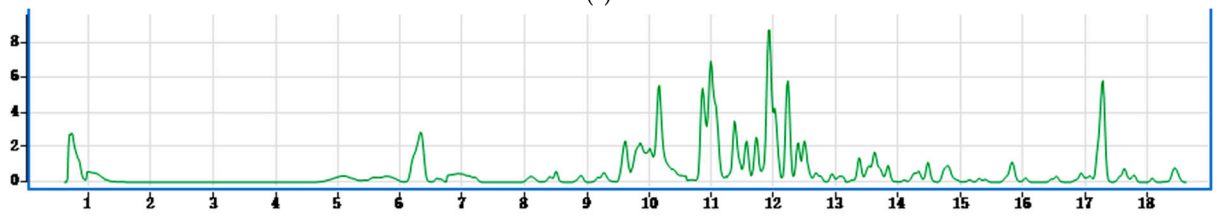

(**II**)

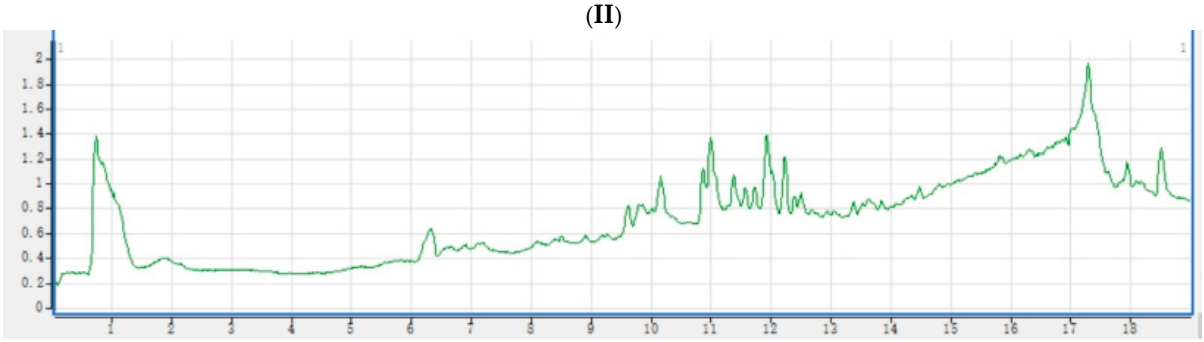

(**III**)

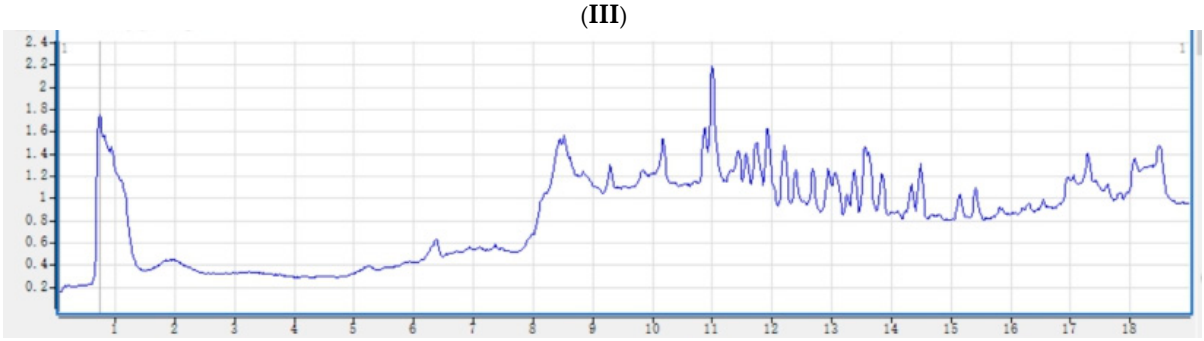

(**IV**)

https://doi.org/10.3390/molecules31234272

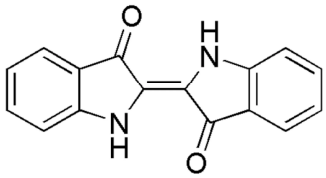

indigo, $C_{16}H_{10}N_2O_2$
m/*z* 263.0815

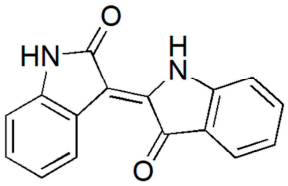

indirubin, $C_{16}H_{10}N_2O_2$
m/*z* 263.0815

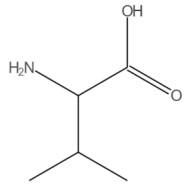

valine, $C_5H_{11}NO_2$
m/*z* 118.0862

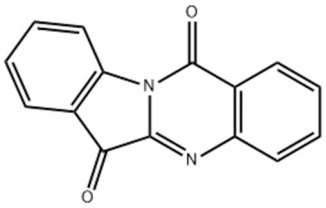

tryptanthrin, $C_{15}H_8N_2O_2$
m/*z* 249.0659

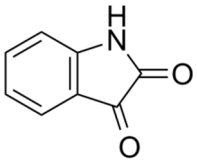

isatin, $C_8H_5NO_2$
m/*z* 148.0393

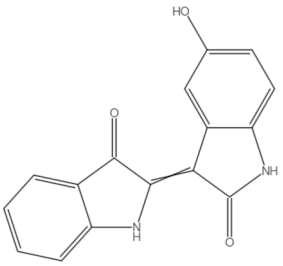

hydroxyindirubin, $C_{16}H_{10}N_2O_3$
m/*z* 279.0764

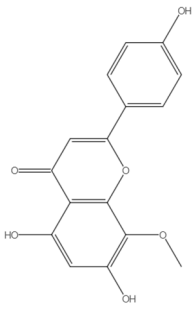

5,7,4′-trihydroxy-8-methoxyflavone,
$C_{16}H_{12}O_6$ *m*/*z* 301.0707

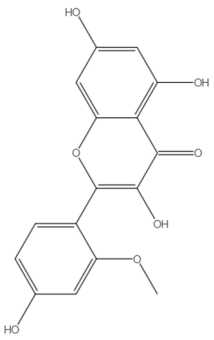

isorhamnetin, $C_{16}H_{12}O_7$
m/*z* 317.0656
(**V**)

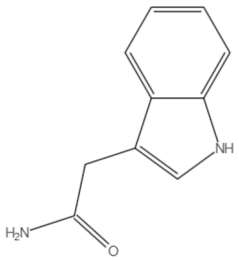

2-(1H-indol-3-yl)acetamide,
$C_{10}H_{10}N_2O$ *m*/*z* 175.0866

Figure 6. (**I**) UPLC profile of SIN (*X*-axis: retention time (min); *Y*-axis: intensity ($\times 10^7$)); (**II**) UPLC profile of NIN (*X*-axis: retention time (min); *Y*-axis: intensity ($\times 10^6$)); (**III**) total ion chromatogram of SIN (*X*-axis: retention time (min); *Y*-axis: intensity ($\times 10^7$)); (**IV**) total ion chromatogram of NIN (*X*-axis: retention time (min); *Y*-axis: intensity ($\times 10^7$)); (**V**) chemical structures of nine common constituents identified in SIN and NIN (the nine shared components detected in both SIN and NIN).

2.8. Solubility Comparison Between NIN and SIN

SIN (1.00 mg) and NIN (1.00 mg) were dissolved in 10 mL of DMF (Figure 7). The color of NIN was significantly darker than that of SIN.

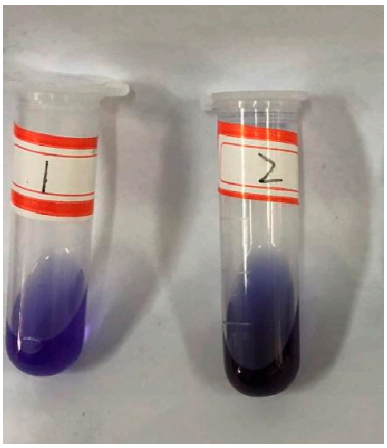

Figure 7. Solubility of NIN and SIN in DMF (1: SIN; 2: NIN, deeper color).

2.9. Quantitative Determination via HPLC

Method validation (n = 5) covering linearity, precision (RSD_{indigo} = 1.35%, $RSD_{indirubin}$ = 1.67%), stability (RSD_{indigo} = 1.69%, $RSD_{indirubin}$ = 1.90%), repeatability (RSD_{indigo} = 0.97%, $RSD_{indirubin}$ = 1.86%) and spike recovery (RSD_{indigo} = 1.06%, $RSD_{indirubin}$ = 1.43%) was completed, and all validation criteria satisfied the analytical requirements. The regression equations were $y_{indigo} = 47.477x + 80.102$ ($R^2 = 0.9996$) for indigo (10–50 μg/mL), and $y_{indirubin} = 51.717x - 10.368$ ($R^2 = 0.9999$) for indirubin (5–25 μg/mL).

The contents of indigo and indirubin across batches are summarized in Table 2. Batch 202001 was prepared without ozone treatment, whereas other batches adopted an ozone-assisted workflow. For NIN batches, the indigo content reached at least 15.63%, and the indirubin content was no less than 6.17%. In comparison, SIN contained merely 2.85% indigo and 0.33% indirubin.

Table 2. Contents of indigo and indirubin in NIN and SIN.

Batch No.	201801	201802	201803	201804	201805	201806	201807	201808	202001	SIN
Indigo (%)	36.05	48.38	51.02	34.13	40.29	49.33	42.30	48.62	15.63	2.85
Indirubin (%)	6.40	12.48	13.55	6.17	14.32	11.57	9.49	10.02	29.24	0.33

2.10. Effects on Viability of PBMCs

Within 0–0.32 mg/mL, neither SIN nor NIN produced obvious cytotoxicity toward normal PBMCs at 24 h, 48 h or 72 h; no statistically significant reduction in cell viability was observed (Figure 8). This suggested that SIN and NIN exhibit low toxicity against normal human cells.

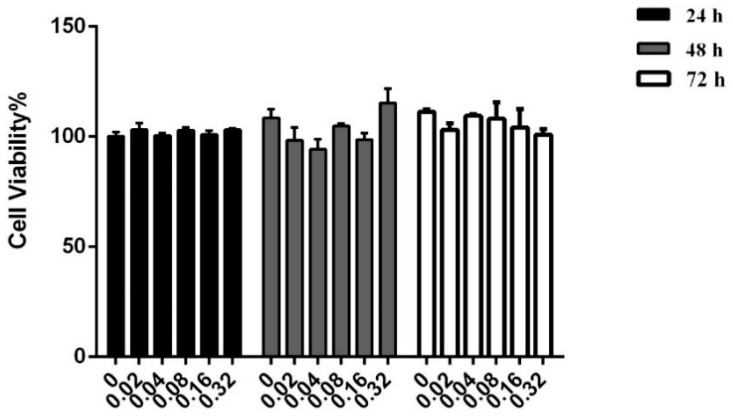

(**A**)

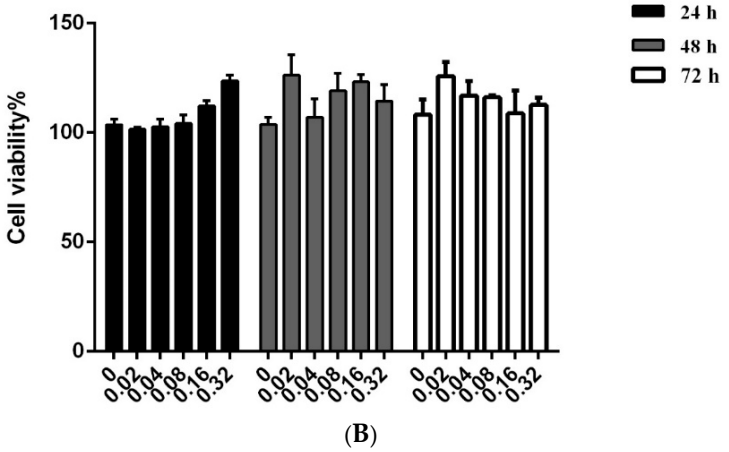

(**B**)

Figure 8. Effects on the viability of PBMCs. (*n* = 3, (**A**) SIN; (**B**) NIN. mg/ML).

2.11. Effects on Viability of K562 Cells

SIN barely inhibited K562 cell proliferation across the whole concentration range at all time points (Figure 9). In contrast, NIN exerted dose-dependent anti-proliferative activity against K562 cells within 0.02–0.32 mg/mL ($p < 0.01$). Cell viability declined more prominently following 48 h and 72 h incubation relative to 24 h treatment.

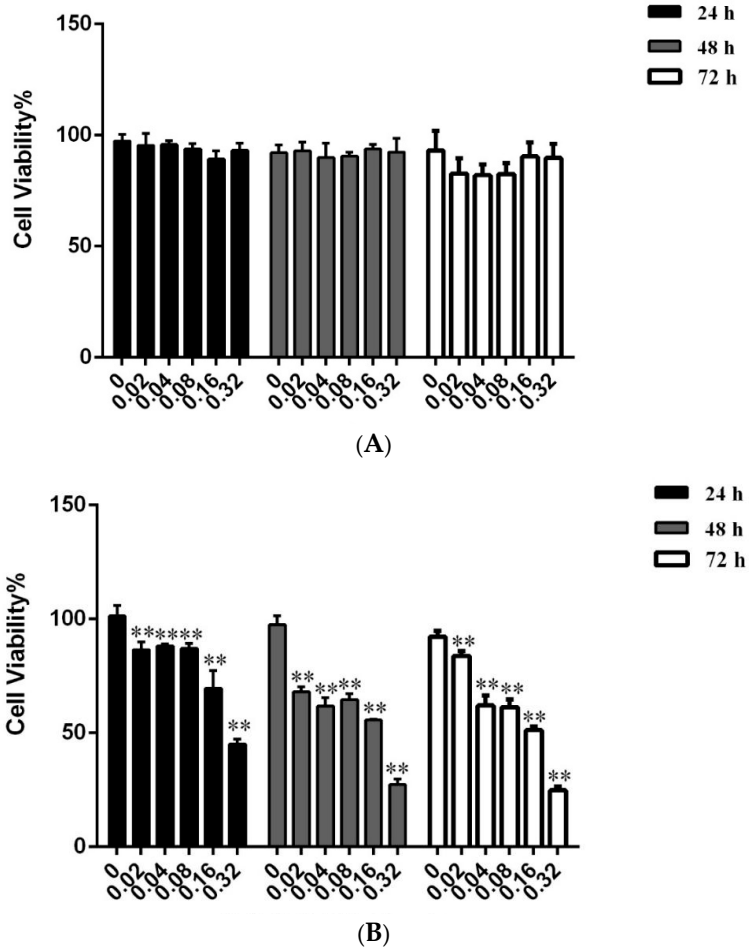

(**A**)

(**B**)

Figure 9. Effects on the viability of K562 cells. (*n* = 3, (**A**) SIN; (**B**) NIN. mg/mL. ** $p < 0.01$ vs. 0 mg/mL group).

2.12. Effects on Viability of HL-60 Cells

SIN showed negligible inhibitory activity against HL-60 cells. NIN could suppress HL-60 cells◎ion growth in a dose-dependent fashion, and this inhibitory effect became more pronounced at 72 h (Figure 10).

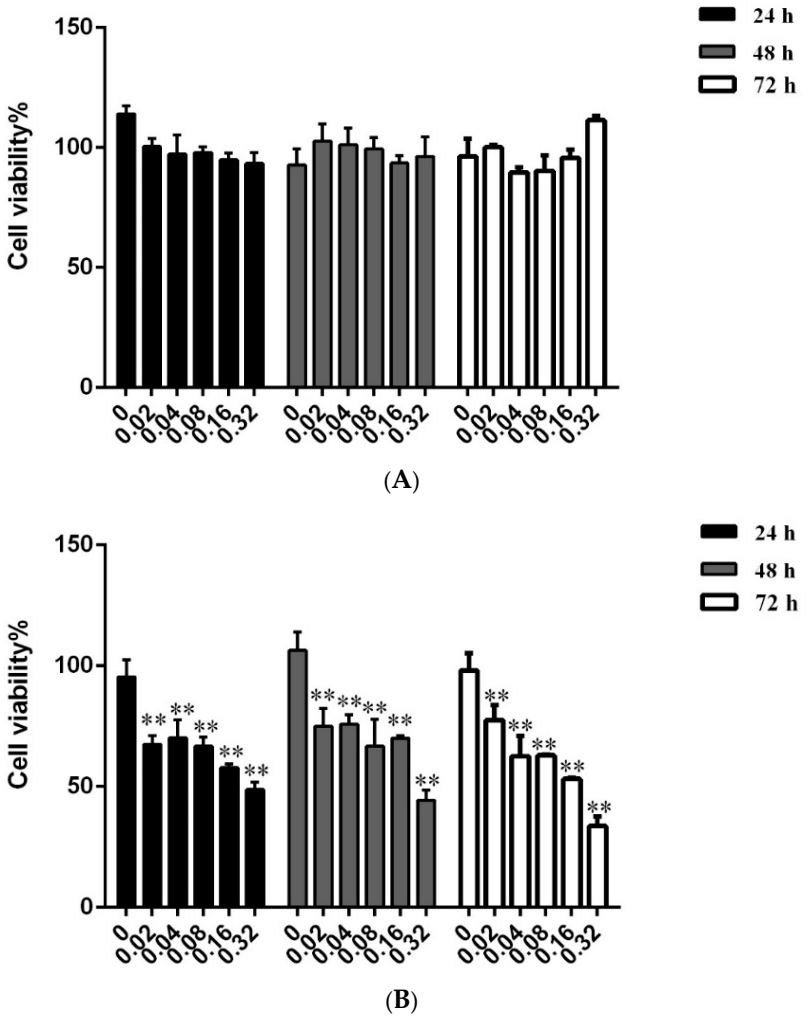

Figure 10. Effects on the viability of HL-60 cells. (n = 3, (**A**) SIN; (**B**) NIN. mg/mL. ** $p < 0.01$ vs. 0 mg/mL group).

2.13. Effects on Viability of SW480 Cells

For SIN, no obvious inhibition was observed at 24 h, while significant cytotoxicity emerged at 48 h and 72 h (0.02–0.32 mg/mL). NIN generated dose-dependent inhibition against SW480 cells at all three time points (Figure 11).

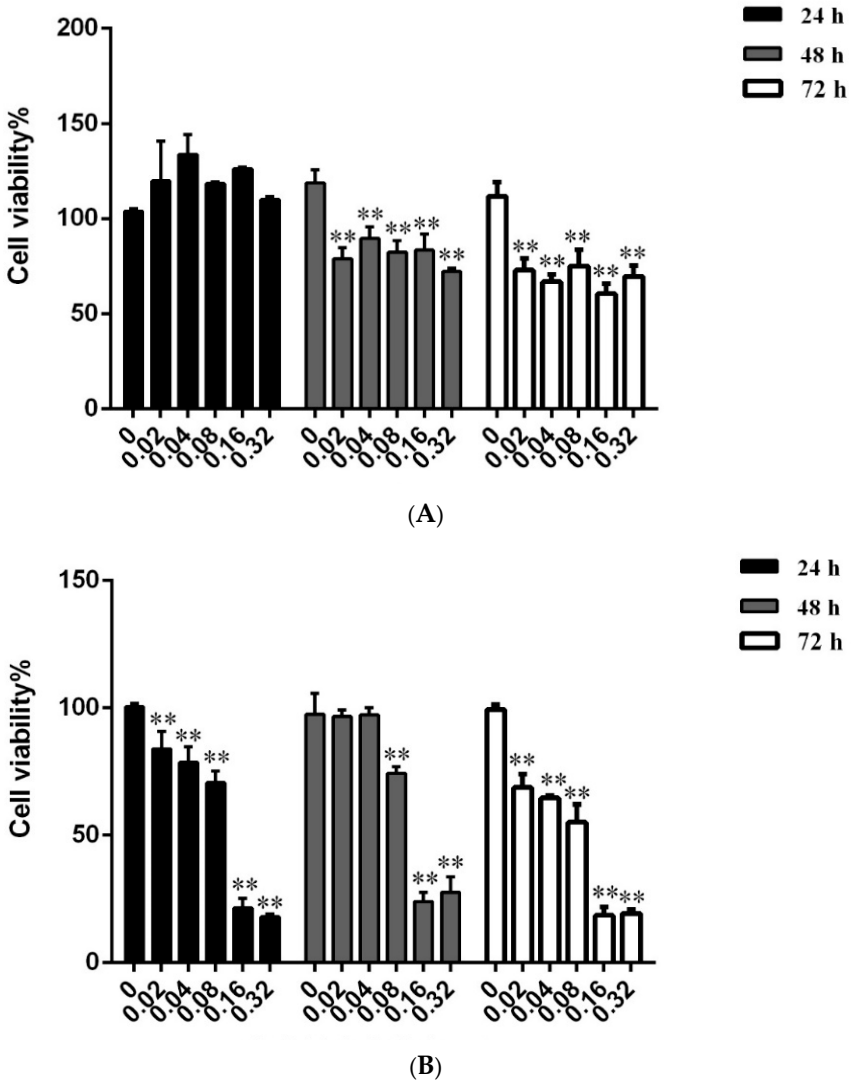

Figure 11. Effects on the viability of SW480 cells. (n = 3, (**A**) SIN; (**B**) NIN. mg/mL. ** $p < 0.01$ vs. 0 mg/mL group).

During conventional IN production, calcium hydroxide used in the soaking procedure generates calcium carbonate precipitates. Combined with inadequate water-grinding steps, the final product suffers from poor quality and lime contamination. Commercial SIN can contain as high as 70% $CaCO_3$ and 10% SiO_2 inorganic impurities [20,21]. After oral administration, these inorganic residues impair therapeutic efficacy and may trigger adverse events such as gastrointestinal hemorrhage [22,23].

The 2020 edition of *Chinese Pharmacopoeia* set minimum limits of ≥2.0% for indigo and ≥0.13% for indirubin in IN. The 2025 version raised these thresholds to ≥3.0% indigo and ≥0.20% indirubin and added the assay for acid-insoluble substances, reflecting increasing regulatory attention toward IN quality control. Our protocol replaces calcium hydroxide with sodium hydroxide, completely avoiding inorganic salt residues; visually, NIN powder exhibits a far deeper color compared with SIN. Relative to SIN, NIN achieves a 10–20-fold elevation in indigo and a 20–30-fold increase in indirubin.

In the concentration range of 0.02–0.32 mg/mL, NIN inhibited the viability of three tumor cell lines in a dose-dependent manner, with maximal effects at 0.16 mg/mL and 0.32 mg/mL. Under identical conditions, SIN only inhibited the viability of SW480 cells, without a detectable effect toward K562 and HL-60. These results suggest that NIN has more pronounced anti-tumor potential than SIN, which may be attributed to its higher

content of the active ingredients than SIN. Further, more rigorous experimental designs are warranted to investigate the anti-tumor activity of NIN.

Nevertheless, the present study bears several limitations. (1) The growth and harvesting cycle of *Baphicacanthus cusia* is seasonal. Further investigations are required to clarify how harvesting season, collection time and processing parameters influence NIN quality and improve batch-to-batch stability. (2) All experiments were performed under laboratory-scale conditions. Process parameters need optimization for large-scale field manufacturing. (3) The NIN and SIN samples themselves have noticeable color. In in vitro assays such as the CCK-8 assay, the color of the drug solution may interfere with the assay. Therefore, concentration-matched cell-free controls and an independent validation assay should be included in future studies. Even so, this lime-free workflow provides valuable references for future IN industrial production.

3. Materials and Methods

3.1. Chemicals and Reagents

Raw medicinal material *Baphicacanthus cusia* (Nees) Bremek. ((psbA-trnH barcode): KT161373.1) was cultivated by the School of Medicine, Huaqiao University. Commercial standard IN (SIN) was purchased from local pharmacies in Quanzhou. Chromatographic-grade methanol was obtained from Xilong Scientific Co., Ltd. (Shantou, China). Analytical-grade N,N-dimethylformamide (DMF) was supplied by Xilong Scientific Co., Ltd. (Shantou, China). Reference standards of indirubin (purity 98.36%) and indigo (purity 98.09%) were purchased from Chengdu Mansite Bio-Technology Co., Ltd. (Chengdu, China). Peripheral blood mononuclear cells (PBMCs) were freshly isolated from the peripheral blood of healthy human volunteers. Human chronic myeloid leukemia K562 cells (CCL-243 (RRID: CVCL_0004)), human acute promyelocytic leukemia HL-60 cells (CCL-240 (RRID: CVCL_0006)) and human colon cancer SW480 cells (CCL-228 (RRID: CVCL_0546)) were obtained from the ATCC (American Type Culture Collection, Manassas, Virginia, USA). The Cell Counting Kit-8 (CCK-8) assay kit was sourced from Shanghai Beyotime Biotechnology Co., Ltd. (Shanghai, China). RPMI-1640 medium, fetal bovine serum (FBS), PBS buffer, and 100 × penicillin–streptomycin stock solution were purchased from Thermo Fisher Scientific (China) Co., Ltd. (Shanghai, China). Dimethyl sulfoxide (DMSO) was supplied by Sinopharm Chemical Reagent Co., Ltd. (Shanghai, China).

3.2. Preparation Process of NIN

NIN was prepared according to previously documented protocols [18,24]. In the follow-up studies of this paper, ozone-prepared NIN was mainly used because it can yield higher levels of indirubin. The NIN batch 201803 was used in in vitro cellular assays. Additionally, considering the convenient field-scale production, we introduced an extra preparation process that does not involve the use of ozone. Fresh leaves of *Baphicacanthus cusia* were collected, washed free of surface contaminants and air-dried. Leaves were stored until partial tissue blackening occurred, then cut into fragments of 1–2 cm. Three hundred grams of leaf fragments was immersed in 3 L of deionized water and subjected to reflux extraction at a constant temperature of 79 °C for 33 min. The mixture was filtered to remove plant residues and the filtrate was retained. One liter of 3.4% hydrochloric acid solution was added to the filtrate for hydrolysis in an 80 °C water bath for 2 h. Subsequently, sodium hydroxide solution was added to adjust pH to 6–8, and the mixture was left to stand overnight. The suspension was centrifuged at 7000 rpm for 5 min at ambient temperature; precipitates were harvested, washed and transferred to evaporating dishes. The supernatant was re-centrifuged to recover residual sediment. Combined

precipitates were dried in an oven at 60 °C overnight, ground into fine powder to yield NIN.

3.3. Combustion Test

A small quantity of NIN powder was placed on aluminum foil and ignited with a mild flame to observe combustion phenomena.

3.4. Nitric Acid Test

NIN powder was placed in a small beaker, concentrated nitric acid was added dropwise, and chemical responses were recorded.

A certain quantity of NIN powder was loaded into a small beaker. Concentrated nitric acid was slowly added dropwise onto the sample powder with gentle shaking. All observable chemical responses, such as color transition, bubble evolution and other visible changes, were closely monitored and documented.

3.5. Moisture Test

Moisture content was measured following the drying method described in the General Chapters of *Chinese Pharmacopoeia*. Briefly, 40.0 mg of sample was spread evenly inside a pre-weighed flat weighing bottle. The open bottle was dried at 100 °C for 5 h, capped, cooled to room temperature in a desiccator for 30 min and weighed accurately. Drying–cooling–weighing cycles were repeated until the mass difference between two consecutive measurements was less than 0.3 mg. Moisture percentage was calculated based on mass loss.

3.6. Water-Soluble Pigment Test

Fifty milligrams of NIN powder was mixed with 10 mL ultrapure water, vortex-shaken and allowed to stand overnight. Color development of the aqueous layer was observed.

3.7. HPLC Fingerprint Analysis

SIN test solution: 20 mg SIN was accurately weighed, approximately 8 mL DMF was added, and ultrasonic extraction was performed for 30 min to achieve complete dissolution. The volume was adjusted to 10 mL with DMF to obtain a 2000 μg/mL test solution, which was filtered through a 0.45 μm microporous membrane prior to injection.

NIN test solution: 1 mg NIN was accurately weighed, approximately 8 mL DMF was added, and ultrasonic extraction was performed for 30 min to achieve complete dissolution. The volume was adjusted to 10 mL with DMF to obtain a 100 μg/mL test solution, which was filtered through a 0.45 μm microporous membrane prior to injection.

HPLC chromatographic conditions: An Elite YWG C18 column (4.6 × 200 mm) was used, with methanol–water as the mobile phase for gradient elution. The elution program is shown in Table 3. The flow rate was 1 mL/min, the detection wavelength was 245 nm, and the injection volume was 20 μL.

For linearity assessment, indirubin standard solutions were serially diluted to final concentrations of 5, 10, 15, 20 and 25 μg/mL; indigo standard solutions were prepared at 10, 20, 30, 40 and 50 μg/mL. Ten microliters of each solution was injected under the above chromatographic settings. Calibration curves were plotted with concentration (μg/mL) as the abscissa and peak area as the ordinate.

Mixed reference working solution: 0.8 mg indigo reference and 0.2 mg indirubin reference were dissolved in ~18 mL DMF with 30 min sonication, brought to 20 mL and filtered through a 0.45 μm membrane.

Table 3. HPLC gradient elution profile.

Time (min)	Methanol (%)	Water (%)
0	10	90
10	20	80
15	30	70
20	50	50
25	55	45
30	60	40
35	70	30
50	75	25
55	80	20
65	90	10
80	90	10

3.8. UPLC-Q-TOF-MS/MS Fingerprint Analysis

UPLC conditions: Chromatographic separation was achieved on an Acquity UPLC BEH C18 column (1.7 μm, Waters, Milford, MA, USA). Methanol–water was adopted as the mobile phase with gradient elution shown in Table 4. Flow rate 0.6 mL/min; column temperature 30 °C; UV detection wavelength 245 nm; and injection volume 10 μL.

Time-of-Flight Mass spectrometry (TOF-MS) parameters: A QTOF-MS detector operating in positive ion electrospray ionization mode. The mass scanning range covered m/z 50–1100. Nitrogen served as drying gas at 11 L/min and 350 °C; nebulizer pressure 45 psig; capillary voltage 4000 V; and fragmentor voltage 120 V.

Sample preparation: For NIN, 0.8 mg powder was transferred into a 10 mL volumetric flask. For SIN, 20 mg powder was weighed. Approximately 8 mL DMF was added to each flask, followed by 30 min sonication. Solutions were brought to volume with DMF.

Table 4. UPLC gradient elution profile.

Time (min)	Phase A (%)	Phase B (%)
0	95	5
2	95	5
10	50	50
17	5	95
19	5	95

3.9. CCK-8 Cell Viability Assay

Logarithmically growing normal human PBMCs and three tumor cell lines (K562, HL-60, SW480) were harvested and adjusted to the appropriate cell densities. Cell suspensions were seeded into 96-well plates at densities of 6×10^4–1×10^5 cells/mL (90 μL per well). Four groups were set: blank control (only complete RPMI-1640 medium without cells); negative control (cells without drug treatment); solvent control (cells treated with the highest concentration of DMSO used in drug groups); and treatment groups exposed to serial concentrations of SIN or NIN. Each group was performed in technical triplicate.

Plates were incubated at 37 °C with 5% CO_2 for 24 h. Ten microliters of drug stock solutions was added to the corresponding wells to generate final concentrations of 0.02, 0.04, 0.08, 0.16 and 0.32 mg/mL. At 24 h, 48 h and 72 h post-treatment, 10 μL CCK-8 reagent was supplemented to each well. After incubation for 1–2 h, absorbance was measured at 450 nm.

Cell viability (CV, %) was calculated according to the formula:

$$CV(\%) = (As - Ab)/(Ac - Ab) \times 100\%$$

A_s: Absorbance of wells containing cells treated with target drug concentrations;
A_c: Absorbance of negative control wells (untreated cells);
A_b: Absorbance of blank control wells (medium only, no cells).

3.10. Statistical Analysis

Chemical constituent profiling was conducted using ChemPattern software v1.0 (CalmScience (Beijing) Technology Co., Ltd. (Beijing China)). Additional data and processing procedures are provided in the Supplementary Materials. GraphPad Prism 6 was used for graph plotting. All data were expressed as mean ± standard deviation. Statistical comparisons were carried out via SPSS 17.0 using one-way ANOVA, followed by Tukey's post hoc test for multiple comparisons. $p < 0.05$ was considered statistically significant. All in vitro experiments were independently repeated three times.

4. Conclusions

This work describes a novel processing technology for Qingdai, establishes characteristic chromatographic fingerprints, identifies nine co-existing chemical constituents, and systematically compares the quality of NIN and SIN. A preliminary quality evaluation framework for NIN was established by integrating macroscopic traits, identification tests, physicochemical inspection, content determination, and fingerprint profiling. Our in vitro anti-tumor assays suggest that NIN may have somewhat greater anti-tumor potential under the tested conditions. Overall, this study provides a practical basis for the quality control and evaluation of NIN and demonstrates the feasibility of the proposed processing strategy for indigo obtention. Further studies should optimize the practical indigo preparation process, clarify its underlying mechanisms, and validate its scalability and robustness to promote its broader application.

Supplementary Materials: The following supporting information can be downloaded at: https://www.mdpi.com/article/10.3390/molecules31234272/s1, PART 1: UPLC-Q-TOF-MS/MS; PART 2: Establishment of HPLC Fingerprint Methodology; PART 3: NIN fingerprint; PART 4: NIN Thin-Layer Chromatography (TLC).

Author Contributions: Conceptualization, X.X. and Y.D.; methodology, X.X. and F.Q.; validation, X.Z. and L.L.; formal analysis, Y.Z.; investigation, X.Z. and L.L.; resources, X.Z. and H.Y.; data curation, X.Z. and L.L.; writing—original draft preparation, X.Z. and X.X.; writing—review and editing, X.X. and X.Z.; supervision, X.H. and H.Y.; project administration, Y.Q.; funding acquisition, Y.D. and X.X. All authors have read and agreed to the published version of the manuscript.

Funding: The Key Science and Technology Project of Quanzhou (Grant No. 2022N024), the National Natural Science Foundation of China (Grant No. U1405215), and the Scientific Research Promotion Program for Young- and Middle-Aged Teachers of Huaqiao University (Grant No. ZQN-PY420).

Data Availability Statement: The original contributions presented in this study are included in the article. Further inquiries can be directed to the corresponding authors.

Conflicts of Interest: The authors declare no conflicts of interest. The funders had no role in the design of the study; in the collection, analyses, or interpretation of data; in the writing of the manuscript; or in the decision to publish the results.

References

1. Zhang, S.; Wang, X.; Chen, W.; Zheng, J.; Wang, C.; Qi, C.; Chen, G.; Niu, L. Indigo Dye: From Ancient Extraction to Green Biomanufacturing. *Biotechnol. Appl. Biochem.* **2026**, *73*, 2532–2550.
2. Shi, Y.; Zhang, L.; Wang, L.; Li, S.; Qiu, Z.; Ding, X.; Wang, Y. Quality blues: Traditional knowledge used for natural indigo identification in southern China. *J. Ethnobiol. Ethnomed.* **2021**, *17*, 25.
3. Yang, Q.-Y.; Zhang, T.; He, Y.-N.; Huang, S.-J.; Deng, X.; Han, L.; Xie, C.-G. From natural dye to herbal medicine: A systematic review of chemical constituents, pharmacological effects and clinical applications of indigo naturalis. *Chin. Med.* **2020**, *15*, 127.
4. Shi, J.; Cui, D.; Yu, L.; Zhang, D.; Gong, Y. Indirubin attenuates DSS-induced colitis in mice and is associated with partial gut microbiota shifts and altered intestinal metabolic profiles. *Food Res. Int.* **2026**, *243*, 120412.
5. Jiang, M.; Zhu, W.; Zheng, Z.; Gu, J.; Liu, K.; Wang, Y.; Zhang, X.; Gong, S. Indigo, An Extract from Indigo Naturalis, Improves Busulfan-Induced Oligoasthenospermia in Mice by Regulating the Testicular Immune Environment. *Comb. Chem. High Throughput Screen.* 2026, *Epub ahead of print*.
6. Ma, K.Y.; Hou, B.L.; Fan, A.Q.; Huang, A.L.; Li, B.R.; Liang, Y.N.; Wang, Z. The mechanism of indigo naturalis and its active ingredients against ulcerative colitis. *Sci. Rep.* **2026**, *16*, 5220.
7. Kim, H.J.; Yang, G.; Lee, J.H. Pharmacokinetics and Acute Safety Evaluation of Tryptanthrin, A Bioactive Constituent of Indigo naturalis, Following Intravenous Administration in Mice. *J. Appl. Toxicol.* **2026**, *46*, 3498–3505.
8. Wu, X.; Chen, X.; Dan, J.; Cao, Y.; Gao, S.; Guo, Z.; Zerbe, P.; Chai, Y.; Diao, Y.; Zhang, L. Characterization of anti-leukemia components from Indigo naturalis using comprehensive two-dimensional K562/cell membrane chromatography and in silico target identification. *Sci. Rep.* **2016**, *6*, 25491.
9. Ozawa, K.; Mori, D.; Hatanaka, A.; Sawano, T.; Nakatani, J.; Ikeya, Y.; Nishizawa, M.; Tanaka, H. Comparison of the anti-colitis activities of Qing Dai/Indigo Naturalis constituents in mice. *J. Pharmacol. Sci.* **2020**, *142*, 148–156.
10. Wang, C.; Yang, P.; Wang, J.; Liu, L.; Chen, J.; Cai, X.; Zhang, M.; Lin, N.; Wang, S.; Yu, Y.; et al. Evidence and potential mechanism of action of indigo naturalis and its active components in the treatment of psoriasis. *Ann. Med.* **2024**, *56*, 2329261.
11. Jiang, Z.; Sun, Y.; Wu, Z.; Tang, M.; Ye, A.; Tu, B.; Yi, J.; Xu, H.; Gao, Y. Dissection of scientific compatibility of Chinese medicinal formula Realgar-Indigo naturalis as an effective treatment for promyelocytic leukemia from the perspective of toxicology. *J. Ethnopharmacol.* **2023**, *317*, 116895.
12. Bai, D.; Zhang, Z.; Gao, J.; Wang, Q.; Macdonald, R.; Xu, Z.; Chen, S.; Huang, N.; Luo, L. Effects of realgar-indigo naturalis formula on a zebrafish tumor xenograft model induced by human acute promyelocytic leukemia cells: Antitumor activity, hepatotoxicity, and transcriptomic analysis. *Front. Pharmacol.* **2025**, *16*, 1619352.
13. Jiang, P.; Sun, D.; Zhang, Y.; Wang, D.; He, J.; Tang, X. Qinghuang powder ameliorates cellular senescence and energy metabolism abnormalities in bone marrow mesenchymal stem cells of myelodysplastic syndromes. *J. Ethnopharmacol.* **2026**, *373*, 122323.
14. Zhao, Y.; Zhong, Y.; Zheng, Q.; Yin, C.Y.; Cai, J.L.; Wang, D.J.; Zhu, L.; Cao, J.; Yan, X.J.; Lian, Y.P. Structural Characterization and Antioxidant Activity of Polysaccharides From Indigo Naturalis *Ophiopogon japonicus*: Effects of Processing and Extraction Methods. *Food Sci. Nutr.* **2026**, *14*, e71522.
15. Ben-Horin, S.; Kopylov, U.; Salomon, N. Curcumin-QingDai Combination as Treatment for Moderate-Severe Ulcerative Colitis. *Case Rep. Gastroenterol.* **2022**, *16*, 563–568.
16. Sugimoto, S.; Naganuma, M.; Kanai, T. Indole compounds may be promising medicines for ulcerative colitis. *J. Gastroenterol.* **2016**, *51*, 853–861.
17. Yu, H.; Li, T.N.; Ran, Q.; Huang, Q.W.; Wang, J. Strobilanthes cusia (Nees) Kuntze, a multifunctional traditional Chinese medicinal plant, and its herbal medicines: A comprehensive review. *J. Ethnopharmacol.* **2021**, *265*, 113325.
18. Xu, X.; Lin, L.; Ning, W.; Zhou, X.; Ullah, A.; Yang, H.; Wu, X.; Diao, Y. Evaluation of Indigo Naturalis Prepared Using a Novel Method: Therapeutic Effects on Experimental Ulcerative Colitis in Mice. *Pharmaceutics* **2025**, *17*, 674.
19. Xu, X.; Lin, L.; Ning, W.; Zhou, X.; Ullah, A.; Huang, X.; Yang, H.; Wu, X.; Diao, Y. Evaluation of Indigo Naturalis Prepared Using a Novel Method: Anti-Inflammatory Activities Against Colonic Cancer Cell Lines. *Mediat. Inflamm.* **2026**, *2026*, 1141244.
20. Xu, Y.; Lin, C.; Tan, H.Y.; Bian, Z.X. The double-edged sword effect of indigo naturalis. *Food Chem. Toxicol.* **2024**, *185*, 114476.
21. Sun, Q.; Leng, J.; Tang, L.; Wang, L.; Fu, C. A Comprehensive Review of the Chemistry, Pharmacokinetics, Pharmacology, Clinical Applications, Adverse Events, and Quality Control of Indigo Naturalis. *Front. Pharmacol.* **2021**, *12*, 664022.

22. Shi, Y.; Wei, F.; Ma, S.C. Discussion on source, preparation and quality of Indigo Naturalis. *China J. Chin. Mater. Med.* **2019**, *44*, 608–613.
23. Seo, Y.; Woo, J. Defined Natural Products as Adjunctive Therapies: Evidence-Gated Polypharmacology Across Molecular Targets, Human Exposure, Clinical Signals, and Safety Boundaries. *Int. J. Mol. Sci.* **2026**, *27*, 7111.
24. Xu, X.; Diao, Y.; Zhou, X. A Preparation Method of Indigo Naturalis. Chinese Patent CN109364126B, 8 October 2021.

Disclaimer/Publisher's Note: The statements, opinions and data contained in all publications are solely those of the individual author(s) and contributor(s) and not of MDPI and/or the editor(s). MDPI and/or the editor(s) disclaim responsibility for any injury to people or property resulting from any ideas, methods, instructions or products referred to in the content.